

# The age and provenance of the Lay Range assemblage provides an indirect record of basement to north-central Quesnellia, British Columbia



Luke Ootes<sup>1, a</sup>, Fil Ferri<sup>1, 2</sup>, Dejan Milidragovic<sup>3</sup>, and Corey Wall<sup>4</sup>

<sup>1</sup> British Columbia Geological Survey, Ministry of Energy, Mines and Low Carbon Innovation, Victoria, BC, V8W 9N3

<sup>2</sup> Retired, 1162 Hadfield Avenue, Victoria, BC, V9A 5N7

<sup>3</sup> Geological Survey of Canada, Vancouver, BC, V6B 5J3

<sup>4</sup> Pacific Centre for Geochemical and Isotopic Research, The University of British Columbia, Earth Sciences Building, Vancouver, BC, V6T 1Z4

<sup>a</sup> corresponding author: Luke.Ootes@gov.bc.ca

Recommended citation: Ootes, L., Ferri, F., Milidragovic, D., and Wall, C., 2022. The age and provenance of the Lay Range assemblage provides an indirect record of basement to north-central Quesnellia, British Columbia. In: Geological Fieldwork 2021, British Columbia Ministry of Energy, Mines and Low Carbon Innovation, British Columbia Geological Survey Paper 2022-01, pp. 31-44.

## Abstract

The Lay Range assemblage, the lowest exposed lithostratigraphic unit of north-central Quesnellia, is separated into lower sedimentary and upper mafic tuff divisions. Fossil and field evidence indicates deposition of the lower sedimentary division during the Late Mississippian to Middle Pennsylvanian and of the upper mafic tuff division during the Middle Pennsylvanian to early Permian. A quartz sandstone and polymictic pebble conglomerate from the lower part of the lower sedimentary division yield detrital zircon U-Pb ages between 360 and 290 Ma (Carboniferous to early Permian), with a range of older detrital zircons from ca. 3600 to 890 Ma (Archean and Proterozoic). A small population of zircons ranges from 450 to 390 Ma (n=4; Ordovician to Devonian). The Carboniferous detrital zircons have mostly juvenile  $\epsilon\text{Hf}(t)$ , indicating that the parental magmas did not interact with older crust. Few zircons are more evolved and were derived from parental magmas that interacted with or melted from crust as old as middle Mesoproterozoic. The combined  $\epsilon\text{Hf}(t)$  and trace element compositions of detrital zircon are consistent with formation in a juvenile arc during the Carboniferous. Comparison of Lay Range detrital zircon U-Pb, Hf, and trace element systematics indicate a similar timing of arc magmatism with eastern Stikinia and Wrangellia, but little relationship to ancient North America or Yukon-Tanana terrane. The older detrital zircons (Archean through Paleozoic) were sourced from a fringing landmass, possibly a continental oceanic plateau, that had little to no role in the petrogenesis of the Carboniferous magmas. The spread of ages in the Lay Range assemblage zircon distributions likely records multiple cycles of deposition, uplift, erosion, transport, and sedimentation. One possibility is that the fringing landmass was calved from the Neoproterozoic through Cambrian western North American passive margin.

**Keywords:** Quesnel terrane, Lay Range assemblage, lower sedimentary division, detrital zircon U-Pb, detrital zircon Hf, detrital zircon trace elements

## 1. Introduction

The Cordilleran orogen of western North America is a type example of an accretionary orogen, but the origin of many terranes (e.g., Quesnellia and Stikinia) remains enigmatic. Paired U-Pb and Lu-Hf isotopic data from detrital zircon provide otherwise inaccessible insights into the origin of source rocks, particularly those that are poorly preserved or unrepresented (e.g., Beranek et al., 2013; Malkowski and Hampton, 2014; Colpron et al., 2015; Pecha et al., 2016; Romero et al., 2020; Alberts et al., 2021; George et al., 2021; Ootes et al., in press). In many cases, detrital zircons from the lowest stratigraphic unit provide the only, and necessarily indirect, record of pre-existing basement upon which a terrane developed (e.g., Ootes et al., in press).

Quesnellia is one of the easternmost terranes of the Cordilleran orogen, commonly juxtaposed directly against rocks of Ancestral North America (Fig. 1). It consists mainly

of a Mesozoic arc complex, represented by Middle Triassic to Early Jurassic volcanic, sedimentary, and intrusive rocks, but locally includes Paleozoic rocks which, in southern British Columbia, are assigned to the arc-like Harper Ranch subterrane and the oceanic Okanagan subterrane (Monger et al., 1991). In north-central British Columbia, Carboniferous to early Permian sedimentary and volcanic rocks, which closely resemble the Harper Ranch subterrane in southern British Columbia, form the basal units of Quesnellia (Monger et al., 1991; Ferri, 1997; Beatty et al., 2006). Subdivided into 'lower sedimentary' and 'upper mafic tuff' divisions (e.g., Ferri, 1997), the Lay Range assemblage has sedimentary features and fossil assemblages that are consistent with a transition from Carboniferous mainly deep-marine sedimentation to early Permian deposition of volcanosedimentary rocks (Ferri, 1997; Ferri et al., 2001).

Presented here are the first detrital zircon U-Pb, Hf, and trace element results from the lower sedimentary division of

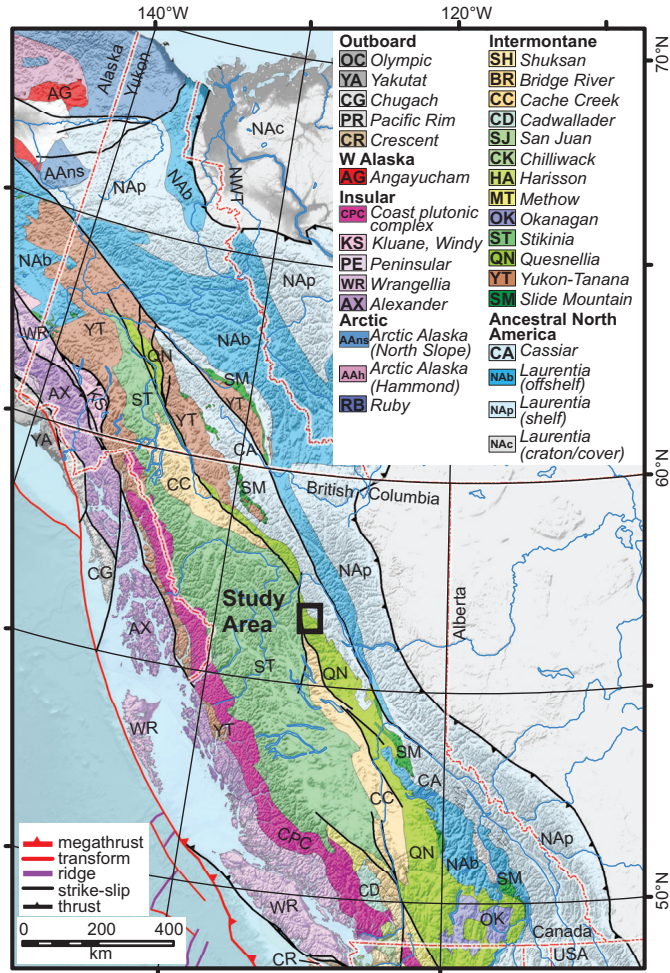


Fig. 1. Terranes of the Cordilleran orogen and location of study. Modified after Colpron (2020).

the Lay Range assemblage in the Lay Range, which is in the traditional territory of the Tsay Keh Dene Band and Takla Lake First Nation. These results offer insights into the age and antiquity of the crust that Quesnellia developed on and allow direct comparison with similar zircon U-Pb and Hf data from Stikinia, Wrangellia, Yukon-Tanana, and cratonic North America. In its north-central segment, Quesnellia was built on an oceanic basement of juvenile volcanic arc rocks formed adjacent to a continental landmass, possibly a block calved during rifting of the western edge of North American crust covered by Neoproterozoic through Cambrian passive margin deposits.

2. Geology of the Lay Range area

The Lay Range assemblage includes Mississippian to Permian sections of predominantly sedimentary and predominantly volcanic rocks (Roots, 1954; Monger, 1973, 1977; Monger and Paterson, 1974; Ross and Monger, 1978). Ferri (1997, 2000) and Ferri et al. (2001) subdivided the Lay Range assemblage into a ‘lower sedimentary division’ and an ‘upper mafic tuff division’ (Fig. 2). Relationships between the two divisions are

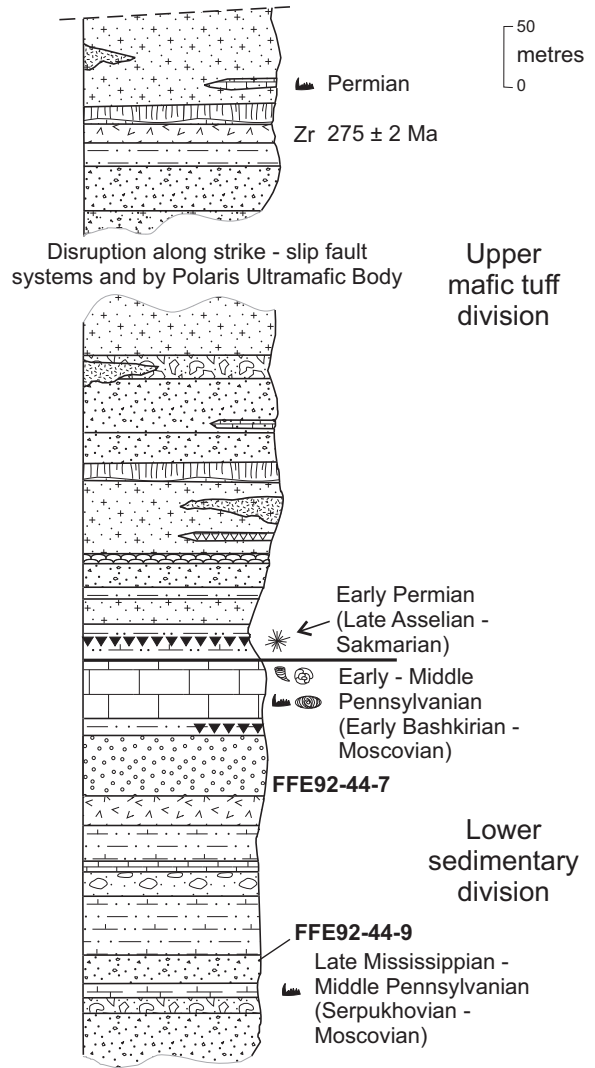


Fig. 2. Composite stratigraphy of the Lay Range assemblage. Modified after Ferri (1997).

best preserved in a northeasterly overturned anticline in the Lay Range mountains (Figs. 3, 4). The core of this southeast-plunging anticline, exposed across a width of about 1 km, contains the lowest rocks of the lower sedimentary division. These include chert, tuff, and siliciclastic and carbonate rocks that are tightly folded and display a strong cleavage. At the top of this succession is a fossiliferous limestone (Lower to Middle Pennsylvanian) that is overlain and underlain by a distinctive unit of maroon argillite and chert (Figs. 2, 3). This marker can be traced along much of the northeastern limb of the anticline and around its hinge zone. On the southwest limb the marker is repeated by a reverse fault but cut off by northwest-trending (strike-slip?) faults (Fig. 4).

The upper mafic tuff division overlies the maroon marker and consists of >2500 m of tuff, volcanic breccia, and volcanic flows (Figs. 2-4). Although radiolarians (fossil locality F<sub>21</sub>, Fig. 3) from the base of this division are early Permian (Table 1), contact relationships with distinctive cherts in the underlying lower sedimentary division indicate continuous deposition, suggesting that the base of the upper mafic tuff division is Middle Pennsylvanian (Ferri, 2000; see below). Fossil and U-Pb geochronology from elsewhere in the unit imply that most of the volcanism defined by this unit is Permian. Southwest of the anticline, the upper mafic tuff division is only exposed across strike for 1-2 km because it is truncated by the Lay Range fault (Fig. 4). The northeast limb of the anticline consists of a 4 km-wide panel of overturned upper mafic tuff division rocks, bounded by an overturned syncline that includes the western margin of the Polaris intrusion (Fig. 3).

### 2.1. Lower sedimentary division

The lower sedimentary division (Figs. 2-4) consists mainly of black and grey argillite and siltstone (Fig. 5), bedded grey chert, thin-bedded arkose and quartz arenite, and chert-pebble conglomerate and breccia. The conglomerates are polymictic (Fig. 5), containing granules to cobbles of varicoloured chert, quartz, argillite, quartzite, carbonate, green tuff, and clinopyroxene-phyric volcanic rock. Less common rocks include fine- to medium-grained white quartz arenite, rhyolitic tuff, shaly or thin-bedded grey limestone, fossiliferous limestone, limy argillite, and green-grey tuffaceous rocks and volcanic sandstones. Minor, small felsic or dioritic intrusions and a narrow serpentinite body are locally in the division.

The top of the division is typically limestone that is up to 75 m thick (Figs. 2, 3). It consists of grey to white, massive to thinly bedded, bioclastic limestone, locally rich in colonial and solitary horn corals, echinoderm, and sponge material, and fusulinaceans and foraminifera (Table 1; F<sub>1</sub> to F<sub>5</sub>, F<sub>8</sub> to F<sub>11</sub>, F<sub>13</sub> to F<sub>15</sub>, F<sub>17</sub> to F<sub>19</sub> in Figure 3). The limestone is locally dolomitic and contains green tuffaceous layers and nodular masses of red or grey chert. At several localities, the limestone is gradationally underlain and overlain by distinctive packages up to 50 m thick of maroon, cream, and grey, thinly bedded argillite, siltstone, and chert (Figs. 2, 3).

### 2.2. Upper mafic tuff division

The most distinctive and widespread rocks of the Lay Range assemblage are green to light green and maroon, mafic volcanic rocks of the upper mafic tuff division (Figs. 2-4). The volcanic rocks include tuffs, flows, and volcanic breccias. Interbedded with the mafic volcanic rocks are subordinate green to grey argillite, siltstone, volcanic wacke and conglomerate, felsic tuff, chert, limy siltstone, and limestone. Mafic flows and large clasts commonly contain clinopyroxene and feldspar phenocrysts and amygdules. Whole rock geochemical data support the interpretation that the volcanic rocks were deposited as part of an arc sequence (Ferri, 1997).

### 2.3. Previous fossil and U-Pb zircon ages

Previous fossil collections and unpublished zircon U-Pb geochronology indicated that the Lay Range assemblage was deposited between the Late Mississippian and Permian (Fig. 2; Table 1). The lower sedimentary division contains Late Mississippian conodonts near the detrital zircon sample locations of this study (Fig. 2; Table 1). The upper limestone of the lower sedimentary division contains Lower to Middle Pennsylvanian (Bashkirian to Moscovian) fusulinids (Fig. 2; Table 1; Ross and Monger, 1978). Other fossils from the lower sedimentary division include corals, foraminifers and fusulinaceans that are Middle Pennsylvanian (Moscovian; Fig. 2; Table 1).

Radiolaria extracted from chert near the base of the upper mafic tuff division indicate it is early Permian (late Asselian to Sakmarian; Fig. 2; Table 1). The chert occurs only a few m above a thin limestone unit that contains Middle Pennsylvanian fusulinids (late Moscovian; Table 1; Ross and Monger, 1978). The contact between the chert and limestone is abrupt but is otherwise unremarkable; given the early Permian age of the chert, it is likely that the underlying limestone is stratigraphically equivalent to the uppermost limestone of the lower sedimentary division. This requires that a reverse fault (possibly a steepened thrust) repeats the lower sedimentary division limestone in this area (Fig. 4). Initially, the abrupt contact between limestone and maroon and green chert was interpreted as an unconformity (Ferri, 1997). However, mapping in the northern Lay Range suggests a gradational contact between limestone and overlying tuffs (Ferri, 2000). This revised interpretation makes the upper mafic tuff division as old as Middle Pennsylvanian. Conodonts are broadly Permian elsewhere in the upper mafic tuff division. The biochronological data are consistent with a 275 ± 2 Ma zircon U-Pb age of a felsic tuff unit within the upper mafic tuff division in the Swannell Range (west of the study area; Ferri, unpublished data).

### 3. Methods

The samples for this study (Table 2) were collected during bedrock mapping (Ferri, 1997; Ferri et al., 2001) and retrieved from the British Columbia Geological Survey archive in 2021. They include a fist-sized quartz-rich sandstone (FFE92-44-7) and a fist-sized polymictic pebble conglomerate (FFE92-44-9;

**Table 1.** Paleontologic data from the Lay Range assemblage. All samples were taken from the lower sedimentary division except map number F21, which is from the upper mafic tuff division. UTM Zone 10, NAD 27.

Map No.	GSC Loc. No.	Field Number (Collector)	UTM X	UTM Y	Fossils	Taxa	Age	CAI	Remarks
F <sub>1</sub>	C-37882	(J.W.H. Monger)	328230	6269750	fusulinids	<i>Pseudoendothyra</i> sp. <i>Profusulinella prisca</i> (Deprat) <i>Profusulinella</i> sp. <i>Fusulinella</i> (?) <i>densa</i> sp.	late early Moscovian (Kashirian) <sup>1</sup>		
F <sub>2</sub>	C-37883	(J.W.H. Monger)	328620	6270370	fusulinids	<i>Pseudoendothyra timanica</i> Rauzer-Chernousova <i>Pseudostaffella gorskyi</i> Grozdilova and Lebedeva	early Moscovian, probably Kashirian <sup>1</sup>		
F <sub>3</sub>	C-37879	(J.W.H. Monger)	328450	6268750	fusulinids	<i>Profusulinella prisca</i> sp. (Deprat) <i>Fusulinella</i> (?) <i>densa</i> sp.	late early Moscovian (Kashirian) <sup>1</sup>		
F <sub>4</sub>	C-37880	(J.W.H. Monger)	327500	6269750	fusulinids	<i>Fusulinella decora</i> sp.	late Moscovian (Myachkovskian) <sup>1</sup>		
F <sub>5</sub>	C-37881	(J.W.H. Monger)	327250	6270100	fusulinids	<i>Fusulinella decora</i> sp.	late Moscovian (Myachkovskian) <sup>1</sup>		
F <sub>6</sub>	C-37884	(J.W.H. Monger)	328200	6270100	fusulinids	<i>Wedekindella</i> cf. <i>W. uralica</i> (Dutkevich) <i>Profusulinella prisca</i> (Deprat)	late early Moscovian (Kashirian) <sup>1</sup>		
F <sub>7</sub>	C-37885	(J.W.H. Monger)	327100	6270470	fusulinids	<i>Profusulinella prisca</i> (Deprat) <i>Fusulinella decora</i> sp. <i>Fusulinella concava</i> sp.	late Moscovian (Myachkovskian) <sup>1</sup>		
F <sub>8</sub>	C-37886	(J.W.H. Monger)	325300	6273120	fusulinids	<i>Wedekindella</i> cf. <i>W. uralica</i> (Dutkevich) <i>Profusulinella prisca</i> (Deprat)	late early Moscovian (Kashirian) <sup>1</sup>		Position assumed to be within upper limestone of lower sedimentary division. UTM's do not correspond to map location as shown within Figure 6 of Ross and Monger (1978).
F <sub>9</sub>	C-37887	(J.W.H. Monger)	329250	6268010	fusulinids	<i>Millerella</i> sp. <i>Eostaffella</i> sp.	early Moscovian, probably Kashirian <sup>1</sup>		
F <sub>10</sub>	C-37888	(J.W.H. Monger)	329990	6267420	fusulinids	<i>Pseudoendothyra timanica</i> Rauzer-Chernousova <i>Pseudostaffella paracompressa</i> Safonova	late early Moscovian (Kashirian) <sup>1</sup>		
F <sub>11</sub>	C-37889	(J.W.H. Monger)	328800	6267820	fusulinids	<i>Profusulinella prisca</i> (Deprat) <i>Profusulinella arta</i> Leontovich	late early Moscovian (Kashirian) <sup>1</sup>		
F <sub>12</sub>	C-37920	(J.W.H. Monger)	326750	6270530	fusulinids	<i>Profusulinella ovata</i> Rauzer-Chernousova <i>Profusulinella prisca</i> (Deprat)	late early Moscovian (Kashirian) <sup>1</sup>		
F <sub>13</sub>	C-189925	CRe92-26-10 (C. Rees)	329350	6268115	corals fusulinaceans	<i>Profusulinella ovata</i> Rauzer-Chernousova <i>Fusulinella decora</i> sp. <i>Fusulinella concava</i> sp. <i>Lithostrotion</i> sp. <i>Dibunophyllum</i> sp. <i>Corwenia</i> sp.	late Moscovian (Myachkovskian) <sup>1</sup> Late Carboniferous, early Bashkirian <sup>2</sup>		
F <sub>14</sub>	C-189926	CRe92-26-8 (C. Rees)	329540	6268255	sponge foraminifers	<i>Pseudostaffella</i> ( <i>Semistaffella</i> ) <i>variabilis</i> Reitlinger <i>Pseudoendothyra</i> sp. indet. <i>Eostaffella</i> sp. indet.	Late Carboniferous, Moscovian, ?Podolian or younger <sup>2</sup>		The foraminifers in this sample are poorly preserved. They are definitely Moscovian in age, and are probably Podolian or younger (late Moscovian).
F <sub>15</sub>	C-189924	CRe92-26-9-1 (C. Rees)	329420	6268225	coral fusulinaceans	<i>dibunophylloid</i> coral indet. <i>Wedekindella</i> sp. cf. <i>W. matura</i> Thompson	Late Carboniferous, Podolian (early late Moscovian) <sup>2</sup>		
F <sub>16</sub>	C-208313	FFe92-44-11 (F. Ferri)	324763	6272330	conodonts, ichthyoliths	ramiform elements (4) <i>Gnathodus</i> sp. cf. <i>G. girnyi</i> Hass 1953 (6)	Early Carboniferous, Serpukhovian <sup>3</sup>	4.5	

**Table 1.** Continued.

F <sub>17</sub>	C-189919	SFD92-41-12 (S.F. Dudka)	328145	6269805	foraminifers	<i>Fusulinella</i> sp. indet. <i>Profusulinella</i> sp. indet.	Late Carboniferous, Moscovian, ?Kashirian (late early Moscovian) or younger <sup>2</sup>	This sample is definitely Moscovian in age, but its exact position within the Moscovian has not been determined.
F <sub>18</sub>	C-208316	SFD92-41-12 (S.F. Dudka)	338749	6268062	conodonts	ramiform elements (8) <i>Adetognathus?</i> sp. (1) <i>Idiognathodus</i> sp. (6) <i>Idiognathoides</i> sp. (11) <i>Neogondolella clarki</i> (Koike 1967) (3) <i>Corwenia</i> sp.	Late Carboniferous, late Bashkirian-Moscovian <sup>3</sup>	4.5-5.5
F <sub>19</sub>	C-189913	SFD92-41-8-3 (S.F. Dudka)	328660	6270250	corals, foraminifers	<i>Profusulinella</i> sp. ex. gr. <i>P. gorskyi</i> (Dutkevich) <i>Profusulinella</i> sp. ex. gr. <i>P. parva</i> (Lee and Chen) <i>Eostaffella</i> sp. ex. gr. <i>E. oblonga</i> Ganelina <i>Pseudendothyra</i> sp. indet. indeterminate	Late Carboniferous, late Bashkirian to early Moscovian <sup>2</sup>	
F <sub>20</sub>	C-189914	SFD92-41-9 (S.F. Dudka)	328555	6270150	echinoderm columnals	<i>Pseudoalibailiella lomentaria</i> Ishiga and Imoto and Jones	Ordovician to recent <sup>2</sup>	
F <sub>21</sub>	C-189933	SFD92-46-2-4 (S.F. Dudka)	374940	6269540	radiolarians	<i>Pseudoalibailiella</i> sp. cf. <i>scalprata</i> Holdsworth	Early Permian; late Asselian to Sakmarian <sup>3</sup>	
F <sub>22</sub>	C-189916	SFD92-41-14 (S.F. Dudka)	327955	6269540	sponge, echinoderm columnals, foraminifers	<i>Quadrimeris</i> sp. <i>Quinqueremis</i> sp. <i>Chaetetes</i> sp. <i>Fusulinella</i> sp.	Late Carboniferous, Moscovian <sup>2</sup>	The sponge, <i>Chaetetes</i> , occurs as clasts in this conglomerate and the foraminifers are in the matrix.

<sup>1</sup>C.A. Ross in Ross and Monger (1978)

<sup>2</sup>W.E. Bamber, Foraminifera by L. Rui Institute of Sedimentary and Petroleum Geology, Geological Survey of Canada; internal reports nos. C4-EWB-1993, Rui-4-1993

<sup>3</sup>F. Cordey, Cordilleran Division, Geological Survey of Canada

**Table 2.** Locations for Lay Range detrital zircon samples. UTM Zone 10, NAD 27.

Sample	UTM X	UTM Y	Rock type
FEE92-44-7	325310	6272547	Sandstone
FEE92-44-9	325148	6272391	Conglomerate

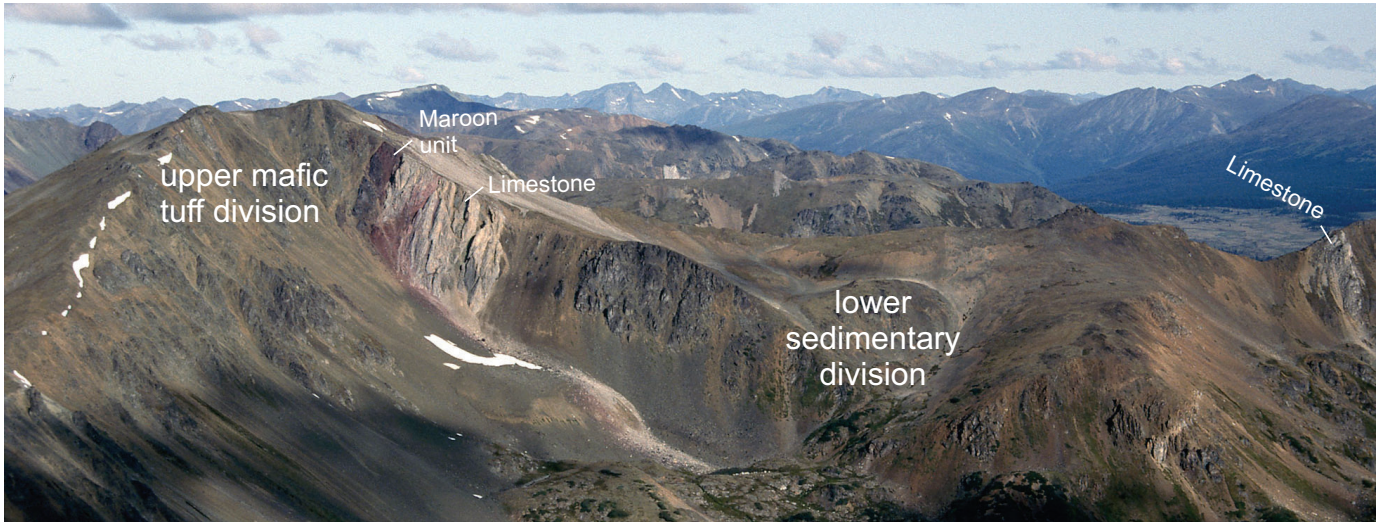


**Fig. 3.** The lower sedimentary and upper mafic tuff divisions of the Lay Range assemblage. In this northwest view, the lower sedimentary division is preserved in the centre of an anticline outlined by pale grey limestone (labelled) on the left and the far right of the photograph. The distinctive maroon sedimentary rocks ('maroon unit') on the left side of the photo (western limb of the fold) are overlain by the upper mafic tuff division.

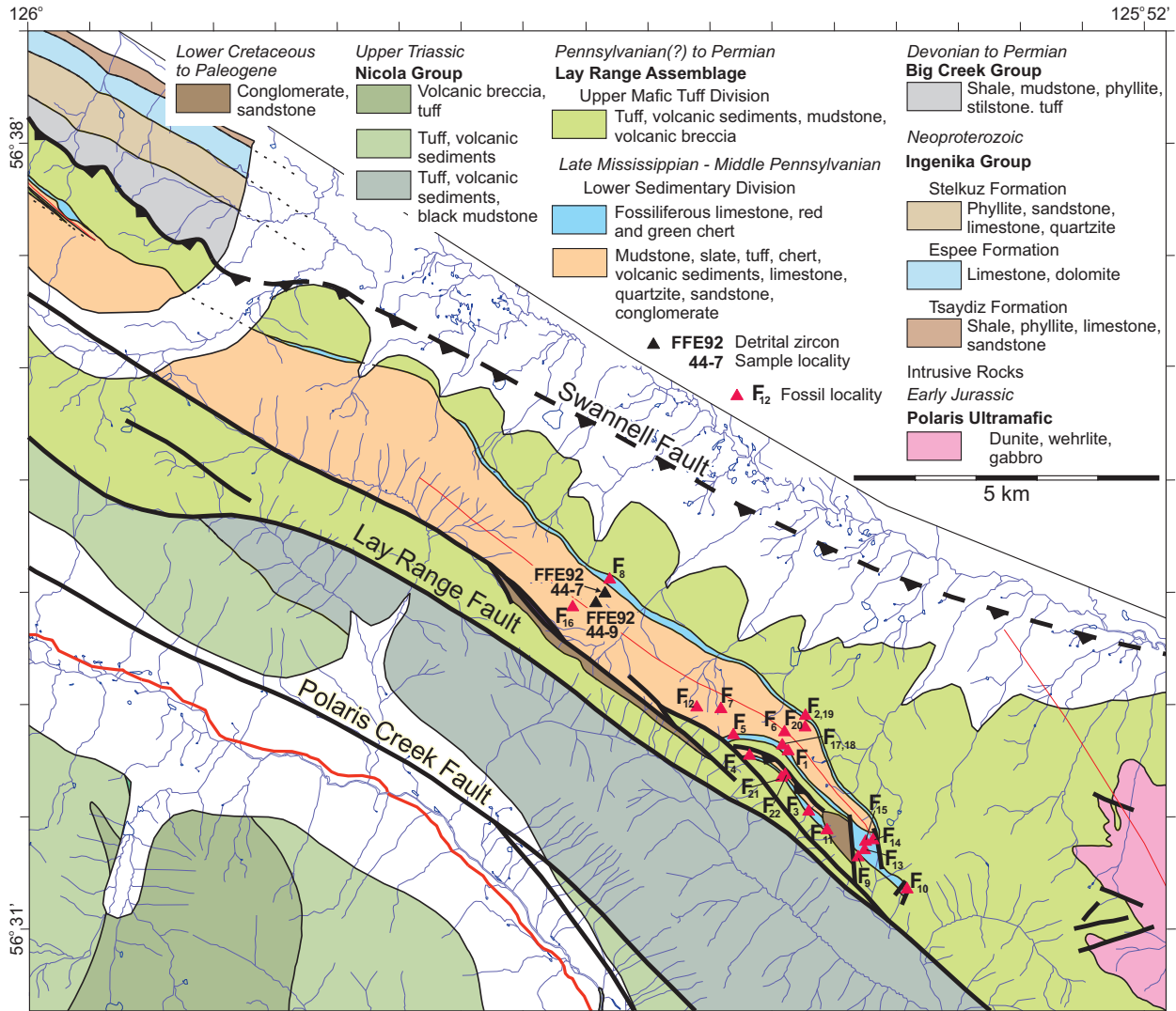


**Fig. 4.** Generalized geology of the study area. After Ferri (1997, 2000) and Ferri et al. (2001).

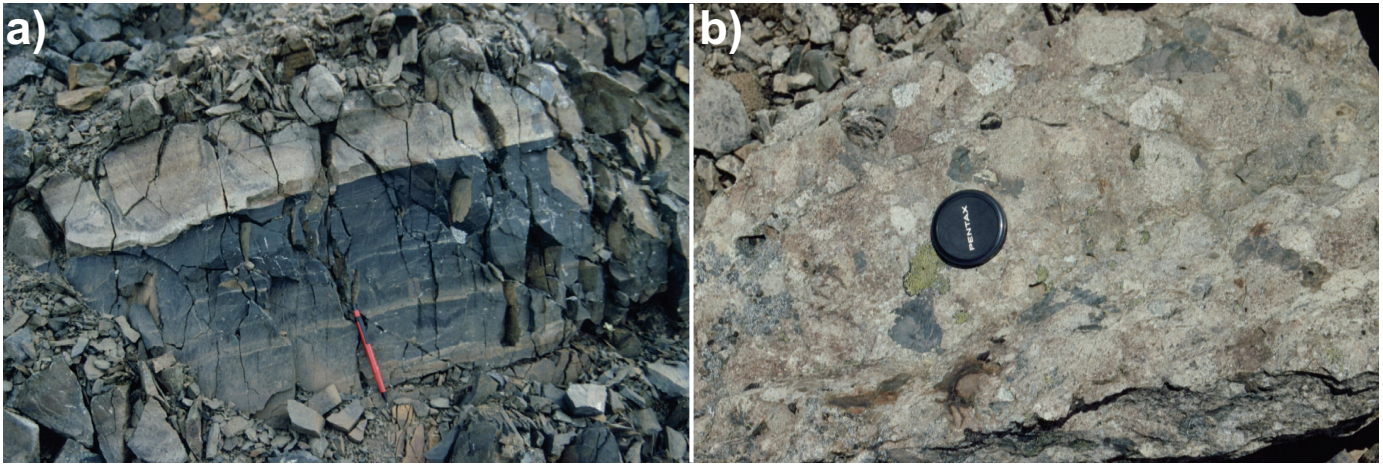


**Fig. 5. a)** Lay Range assemblage, lower sedimentary division. At bottom of photo, sharp-based Bouma-like fining upward sequences of graded siltstones to dark grey argillites. **b)** Lay Range assemblage lower sedimentary division. Polymictic conglomerate with subangular to subrounded chert and volcanic clasts.

Table 2) from the lower sedimentary division (Figs. 2, 4); full analytical techniques, zircon images, and results are provided in supplementary datafiles (Ootes et al., 2022).

Detrital zircon U-Pb/Hf and trace element analyses were acquired at the Pacific Centre for Isotopic and Geochemical Research at the University of British Columbia. Sample FFE92-44-7 yielded a minor amount of zircon (17) whereas sample FFE92-44-9 yielded a large number (>200) of relatively large zircon crystals (>75  $\mu\text{m}$ ) from conventional density and magnetic mineral separation methods. The entire zircon separate was placed in a muffle furnace at 900°C for 60 hours in quartz beakers to anneal minor radiation damage. Annealing enhances cathodoluminescence (CL) emission (Nasdala et al., 2002) and promotes more reproducible inter-element fractionation during laser ablation inductively coupled plasma mass spectrometry (LA-ICPMS; Allen and Campbell, 2012). Following annealing, individual grains were hand-picked and mounted, polished, and imaged by cathodoluminescence (CL) on a scanning electron microscope. From these compiled images, grains with consistent and clear CL patterns were selected for further isotopic analysis.

Analyses were conducted using a Resonetics RESOLUTION M-50-LR, which contains a Class I laser device equipped with a UV excimer laser source (Coherent COMPex Pro 110, 193 nm, pulse width of 4 ns) and a two-volume cell designed and developed by Laurin Technic Pty. Ltd. (Australia). The laser cell was connected via a Teflon squid to an Agilent 7700x quadrupole ICP-MS. A pre-ablation shot was used to ensure that the spot area on grain surface was free of contamination. Samples and reference materials were analyzed for 36 isotopes:  $^7\text{Li}$ ,  $^{29}\text{Si}$ ,  $^{31}\text{P}$ ,  $^{43}\text{Ca}$ ,  $^{45}\text{Sc}$ ,  $^{49}\text{Ti}$ , Fe ( $^{56}\text{Fe}$ ,  $^{57}\text{Fe}$ ),  $^{89}\text{Y}$ ,  $^{91}\text{Zr}$ ,  $^{93}\text{Nb}$ , Mo ( $^{95}\text{Mo}$ ,  $^{98}\text{Mo}$ ),  $^{139}\text{La}$ ,  $^{140}\text{Ce}$ ,  $^{141}\text{Pr}$ ,  $^{146}\text{Nd}$ ,  $^{147}\text{Sm}$ ,  $^{153}\text{Eu}$ ,  $^{157}\text{Gd}$ ,  $^{159}\text{Tb}$ ,  $^{163}\text{Dy}$ ,  $^{165}\text{Ho}$ ,  $^{166}\text{Er}$ ,  $^{169}\text{Tm}$ ,  $^{172}\text{Lu}$ ,  $^{177}\text{Hf}$ ,  $^{181}\text{Ta}$ ,  $^{202}\text{Hg}$ , Pb ( $^{204}\text{Pb}$ ,  $^{206}\text{Pb}$ ,  $^{207}\text{Pb}$ ,  $^{208}\text{Pb}$ ),  $^{232}\text{Th}$ , and U ( $^{235}\text{U}$ ,  $^{238}\text{U}$ ) with a dwell time of 0.02 seconds for each isotope. Pb/U and Pb/Pb ratios were determined on the same spots along with trace element concentration determinations. The settings included a

spot size of 34  $\mu\text{m}$  with a total ablation time of 30 seconds, frequency of 5 Hz, fluence of 5  $\text{J}/\text{cm}^2$ , power of 7.8 mJ after attenuation, pit depths of approximately 15  $\mu\text{m}$ , He flow rate of 800 mL/min,  $\text{N}_2$  flow rate of 2 mL/min., and a carrier gas (Ar) flow rate of 0.57 L/min.

Data were reduced using Iolite 4 software using the UPb\_Geochronology and TraceElements\_IS data reduction schemes (Paton et al., 2011). After detrital zircon U-Pb and trace element analyses, zircon grains were analyzed for Lu-Hf isotopic composition. Lutetium-Hafnium isotope analyses were completed on 32 of the zircons at PCIGR using a New Wave Research, 193nm laser ablation and a Nu Plasma (NP021) MC-ICP-MS on similar CL zones as the U-Pb and trace element analyses. Data were reduced using Iolite 4 software (Paton et al., 2011) using the Hf\_Isotopes data reduction scheme (Woodhead et al., 2004). Uncertainties on initial Hf ratios were propagated through Iolite and epsilon Hf values were calculated using full error propagation, outlined by Ickert (2013).

#### 4. Results

Full analytical results upon which the following is summarized are provided as supplementary datafiles (Ootes et al., 2022). Sixteen detrital zircons from the quartz-rich sandstone sample (FFE92-44-7) were analyzed. Fourteen zircons yield Carboniferous dates (ca. 343 to 308 Ma) with a peak distribution at ca. 330 Ma (Figs. 6a, b). The youngest single zircon has a  $^{206}\text{Pb}/^{238}\text{U}$  date of  $306.4 \pm 10.8$  Ma. The youngest statistical population (Coutts et al., 2019; Harriott et al., 2019) has a weighted mean of  $325.1 \pm 4.2$  Ma ( $n=5$ ;  $\text{MSWD}=0.63$ ), interpreted as the maximum deposition age of the sample. Two zircons have concordia ages of 1660 Ma and 1145 Ma. The Carboniferous zircons have a range of  $\epsilon\text{Hf}(t)$  from -1.5 to +20.5 ( $\pm 3.5$ ; error reported as  $2\sigma$ ; Fig. 5a). The single Precambrian zircon analyzed for Lu-Hf isotopic composition has  $\epsilon\text{Hf}(t) + 6.85$ .

One hundred and nine detrital zircons from the polymictic pebble conglomerate sample (FFE92-44-9) were analyzed.

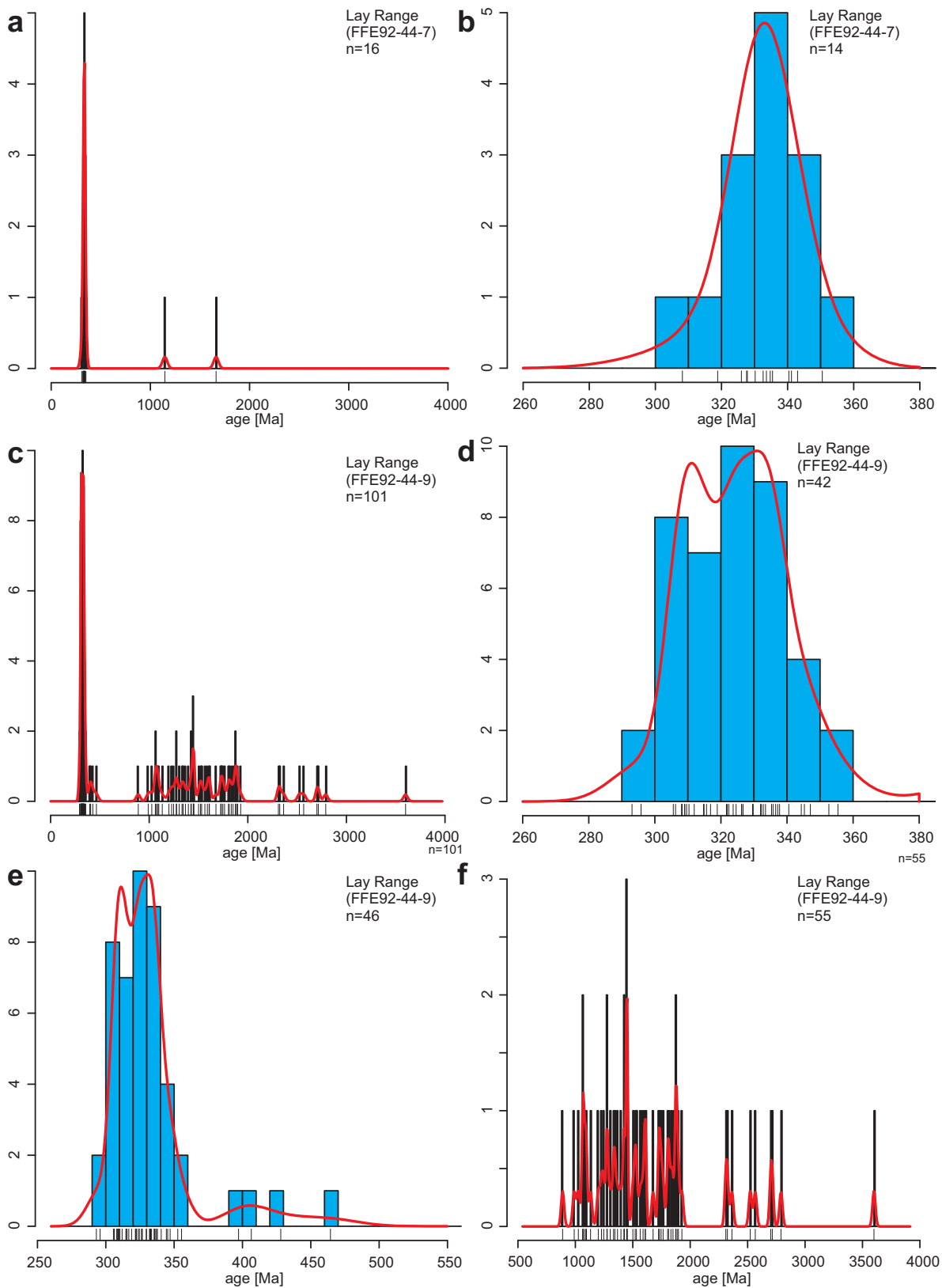


**Fig. 6.** Kernel density estimation (KDE) plots of detrital zircon U-Pb results from a, b) Lay Range samples FFE92-44-7 (quartz-rich sandstone, several 100 m up section) and c-f) FFE92-44-9 (polymictic conglomerate, near the base of the section). **a)** All results and **b)** Carboniferous results from FFE92-44-7. **c)** All results, **d)** Carboniferous and Permian results, **e)** all Paleozoic results, and **f)** Precambrian results from FFE92-44-9. Histogram bin widths are 10 Ma, corresponding to typical uncertainty of individual zircon U-Pb LA-ICP-MS results. Vertical ticks below the probability curves represent single zircon dates (no uncertainty). Data plotted using IsoplotR (Vermeesch, 2018).

After data reduction, P and Ti concentrations in zircon were used to qualitatively screen the data. Eight analyses were removed from the dataset because they have anomalous trace element values (Figs. 7a-c). One hundred and one analyses remained after trace element screening, indicating that ~7% of laser ablation analyses intersected mineral inclusions of apatite, titanite, or other minerals during analysis. This method independently identified analyses that have REE not typical of zircon (Fig. 7d).

Zircon grains from sample FFE92-44-9 yielded a spectrum of U-Pb ages from 3600 to 290 Ma (Fig. 6c). Forty-two zircons have  $^{206}\text{Pb}/^{238}\text{U}$  dates between 360 and 290 Ma (Carboniferous to early Permian; Fig. 6d). The youngest single zircon has a  $^{206}\text{Pb}/^{238}\text{U}$  date of  $293.8 \pm 12.8$  Ma and the youngest statistical population (Coutts et al., 2019; Harriott et al., 2019) has a weighted mean of  $309.4 \pm 2.7$  Ma ( $n=16$ ; MSWD=0.98). This is interpreted as the maximum deposition age of the sample. Four of the zircons have unique (non-overlapping)  $^{206}\text{Pb}/^{238}\text{U}$  dates from 450 to 390 Ma (Paleozoic; Fig. 6e). Fifty-five of the zircons have ages that range from 3600 to 890 Ma (Precambrian; Fig. 6f). The Carboniferous zircons have a range of  $\epsilon\text{Hf}(t)$  from -6.1 to +21.9 (Fig. 8). The four Paleozoic and the Precambrian zircons have  $\epsilon\text{Hf}(t)$  that range from -12.3 to +13.1 and -30 to +14, respectively.

## 5. Discussion

### 5.1. Age of the lower sedimentary division, Lay Range assemblage

Fossils preserved in the lower sedimentary division of the Lay Range assemblage are interpreted to be mostly Middle Pennsylvanian (Moscovian; 315 to 307 Ma; Table 1), but locally are as old as Late Mississippian (Serpukhovian, 331 to 323 Ma). The detrital zircon results are consistent with this interpretation, indicating maximum deposition ages between 310 to 325 Ma (Fig. 6). Nearly half (48%) of the detrital zircons from the lower sedimentary division have Carboniferous ages. A comparison of these ages with those from a quartz arenite sample from the Asitka Group, eastern Stikinia (ca. 290 Ma; Ootes et al., in press), shows strong similarities with central peaks at ca. 320 to 325 Ma (Fig. 9). Two-component finite unmixing yields nearly identical results with age peaks at ca. 315 Ma and 335-340 Ma (Fig. 9). The distribution of Carboniferous U-Pb results is broadly comparable to results reported by Mortensen et al. (2017) from the Okanagan subterrane in southern Quenesllia, British Columbia and Washington State, particularly from the Independence-Bradshaw assemblage, the Oregon claims formation, Ashnola River greywacke, the Barslow assemblage, the Attwood conglomerate, and the Anarchist gneiss; a more detailed statistical comparison cannot be carried out because raw data were not presented.

### 5.2. Detrital zircon $\epsilon\text{Hf}(t)$ and trace elements, lower sedimentary division

Most  $\epsilon\text{Hf}(t)$  values from Carboniferous detrital zircons of the Lay Range assemblage indicate that the parental magmas

were derived from a juvenile source and lacked interaction with ancient crust (Fig. 8a). A subpopulation of the Carboniferous zircon ( $n=6$ ) and three of the older Paleozoic zircons have slightly more evolved  $\epsilon\text{Hf}(t)$  (Fig. 8), indicating parental magmas with an enriched (crustal) component as old as middle Mesoproterozoic to Neoproterozoic; there is little evidence that the magmas yielding the Carboniferous zircons interacted with crust older than Mesoproterozoic (Fig. 8b).

Grimes et al. (2015) used igneous zircon trace elements from a number of tectonic environments to define end-member arc, mid-ocean ridge, and ocean island discrimination fields. Using one of these examples (Nb/Yb vs. U/Yb; Fig. 10), the Lay Range assemblage and Asitka Group (eastern Stikinia) Carboniferous detrital zircons overlap the magmatic arc array and mid-ocean ridge basalt (MORB) fields, but consistently plot above the mantle zircon array defined by MORB and ocean islands (Fig. 10; Grimes et al., 2015). Combined, the trace elements and juvenile  $\epsilon\text{Hf}(t)$  indicate the zircons crystallized in primitive ocean arc-like magmas.

### 5.3. Comparison to Yukon-Tanana terrane, eastern Stikinia, and Wrangellia

The Carboniferous detrital zircon population from the Lay Range assemblage is distinct from that of the Yukon-Tanana terrane (Alaska), which has abundant juvenile to highly evolved detrital zircons of Ordovician to Devonian age (Figs. 8b, c; Pecha et al., 2016). In contrast, the U-Pb and Hf systematics of Carboniferous detrital zircons from the Lay Range assemblage overlap those from eastern Stikinia (Asitka Group; Ootes et al., in press) and Wrangellia (Figs. 8c, 11).

### 5.4. Provenance of detrital zircons in the lower sedimentary division, Lay Range assemblage, and Carboniferous paleogeography

With maximum depositional ages of 325-310 Ma, the lower sedimentary division of the Lay Range assemblage accumulated mainly in a deep-marine depocentre after the start of juvenile arc magmatism. By ca. 300 Ma (the maximum depositional age of the upper mafic tuff division) volcanic tuffs and flows from juvenile arc magmatism overwhelmed background sedimentation. However, although the Lay Range deposits contain mainly Carboniferous detrital zircons, they also contain a high proportion of Precambrian grains (Figs. 6, 8, 11). These grains indicate that erosion of a significantly older crustal landmass also supplied sediment. In addition, although first-cycle quartz sands can be produced by intense tropical weathering of diverse source rocks (e.g., Johnsson et al., 1991), compositionally mature sandstones in the lower sedimentary subdivision are consistent with a continental landmass (Ferri, 1997, 2000). How then can an oceanic arc, with magma sources showing evidence of minimal crustal contribution contain zircons eroded from continental crust?

We suggest that the Lay Range assemblage was deposited peripheral to a continental oceanic plateau (see Ben-Avraham and Nur, 1983) that was isolated in an oceanic setting after

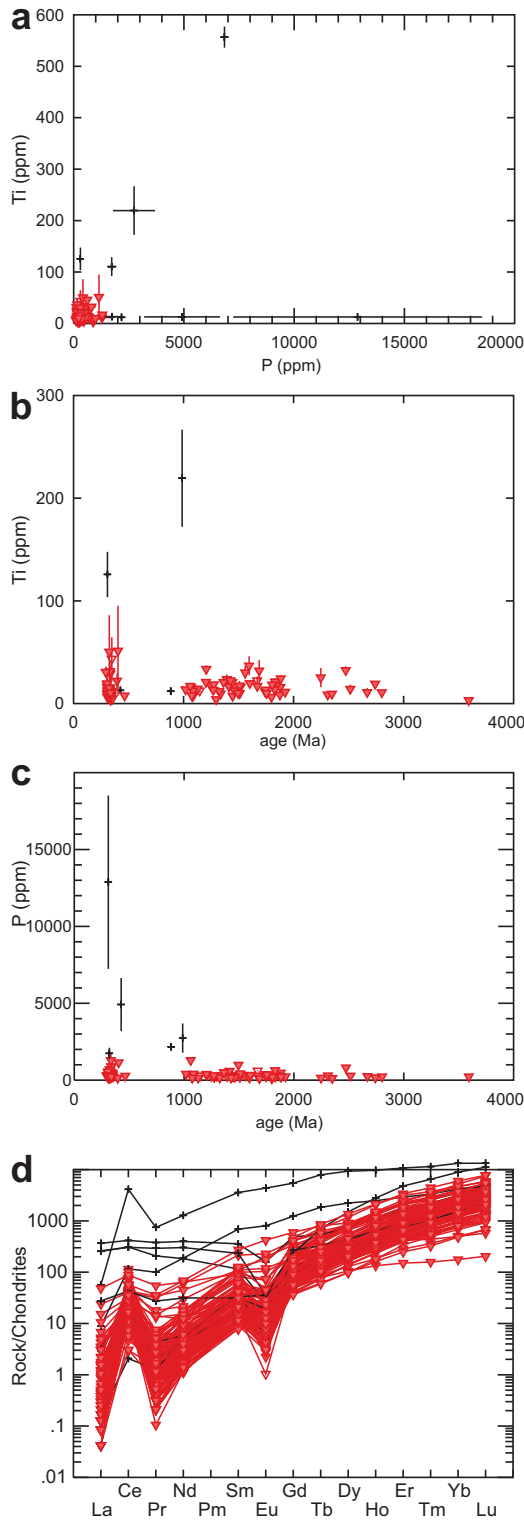


**Fig. 7.** Zircon trace element plots. **a)** P (ppm) vs. Ti (ppm), **b)** age (Ma) vs. Ti (ppm). **c)** age (Ma) vs. P (ppm). Red triangles are data with 'normal' trace element compositions. Black symbols (n=8) are data that were qualitatively identified as outliers whose trace element contents are inconsistent with zircon alone. **d)** Chondrite-normalized (Sun and McDonough, 1989) rare earth element concentrations in zircon. Black symbols were independently identified by qualitative observations in (a-c) and removed from the dataset. Most black symbols have REE profiles that are inconsistent with zircon (red triangles).

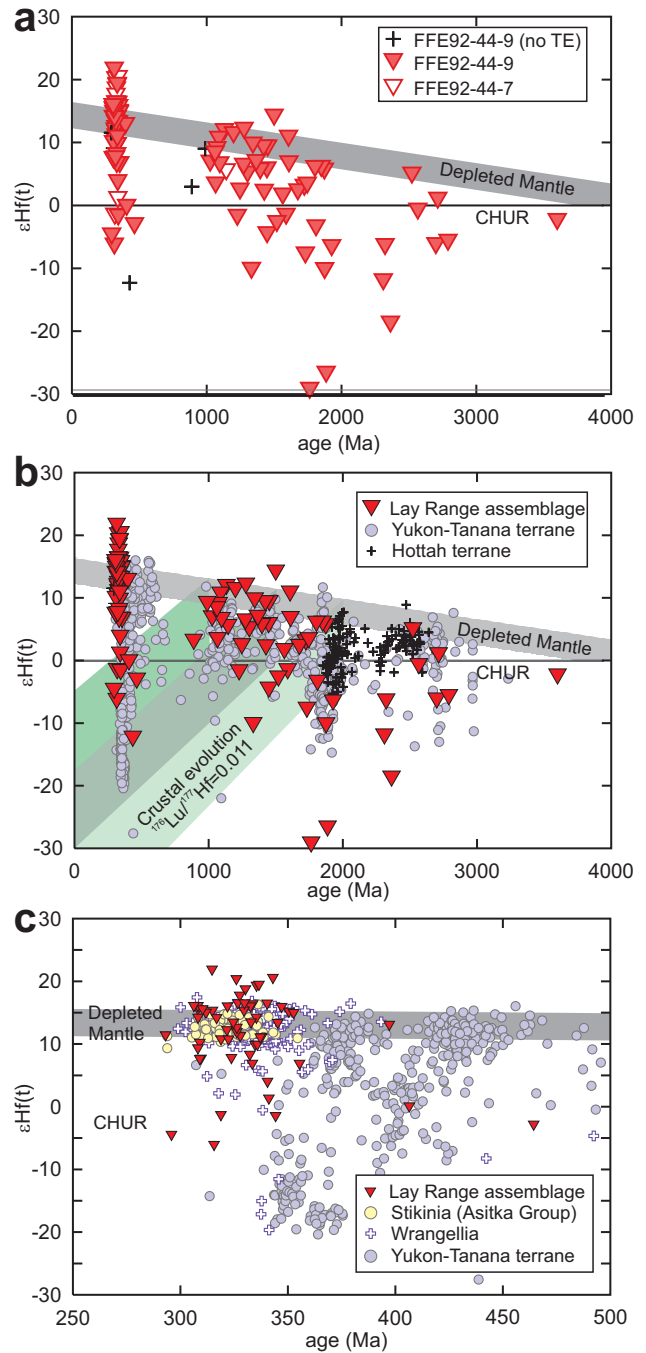


**Fig. 8.** Zircon U-Pb age vs.  $\epsilon\text{Hf}(t)$ . **a)** Detrital zircon data from the Lay Range assemblage, this study. Samples labelled 'no TE' do not have trace element data and therefore were not independently screened. Depleted Mantle curve from Chauvel and Blichert-Toft (2001). Chondrite uniform reservoir (CHUR) from Bouvier et al. (2008). **b)** Comparison of data from the Lay Range assemblage to detrital zircon data from the Yukon-Tanana terrane (Alaska; Pecha et al., 2016) and Hottah terrane, which represents >1900 Ma western Laurentia (Davis et al., 2015). Crustal evolution curves calculated using maximum and minimum Depleted Mantle values at 1000, 1500, and 2000 Ma and assuming  $^{176}\text{Lu}/^{177}\text{Hf}=0.011$  (continental crust; Vervoort and Kemp, 2016). **c)** Comparison of Paleozoic detrital zircons from the Lay Range assemblage with data from the Yukon-Tanana terrane (Pecha et al., 2016), Wrangellia (Alberts et al., 2021; Malkowski and Hampton, 2014; Romero et al., 2020), and Stikinia (Ootes et al., in press).

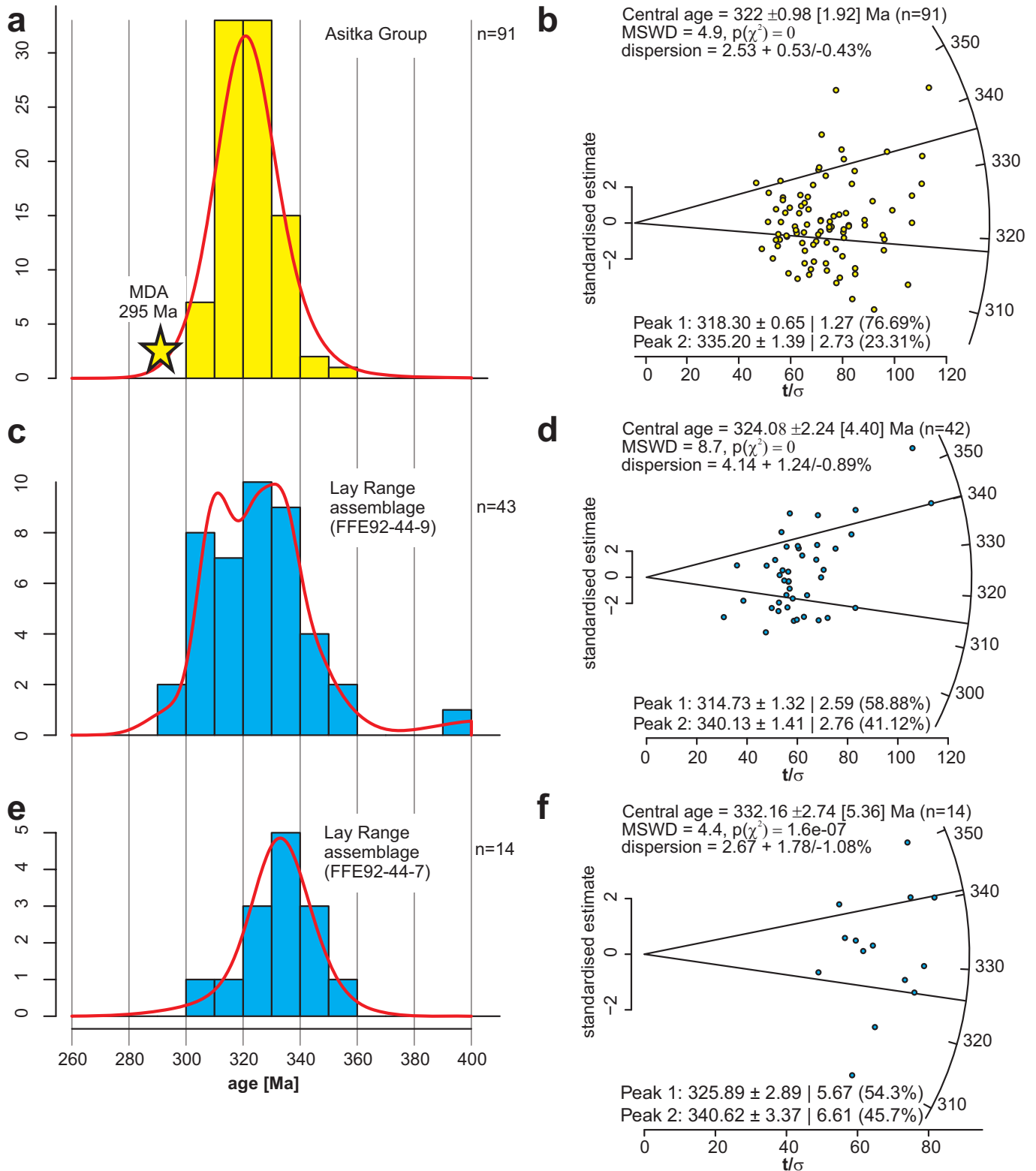


**Fig. 9.** Comparison of Carboniferous detrital zircon ages from Late Paleozoic rocks of the Asitka Group (eastern Stikinia) and the Lay Range assemblage. **a), c), e)** Kernel density element (KDE) plots. Maximum deposition age (MDA) for the Asitka Group determined from zircon U-Pb dating of rhyolite (Ootes et al., in press). Histogram bin widths are 10 Ma, corresponding to typical uncertainty of individual zircon U-Pb LA-ICP-MS results. **b), d), f)** Radial plots that correspond to the adjacent KDE plot. Shown are central ages (MSWD=mean square of weighted deviates). Peak 1 and Peak 2 are the result of finite unmixing models (two component) for each sample set. Data plotted using IsoplotR (Vermeesch, 2018). Data from eastern Stikinia (Asitka Group) are from Ootes et al. (in press).

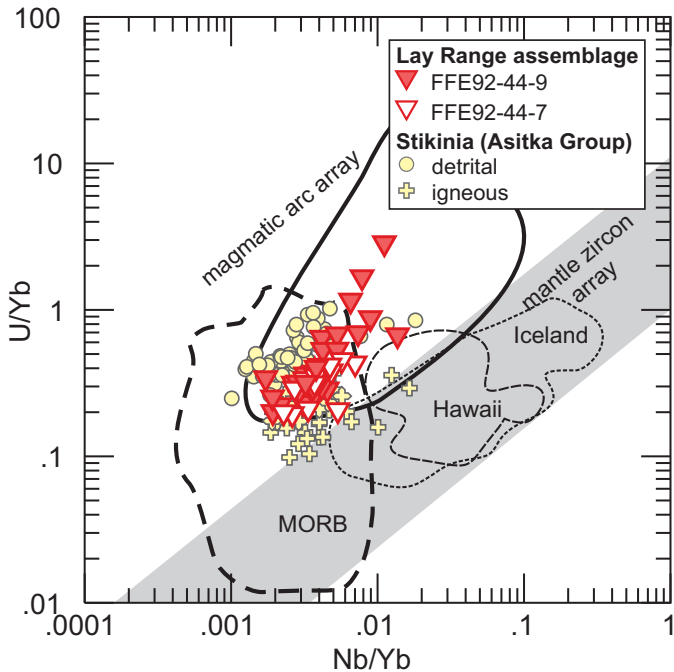


**Fig. 10.** Zircon Nb/Yb vs. U/Yb discrimination diagram (after Grimes et al., 2015) for detrital zircons from the Lay Range assemblage and detrital and igneous zircons from eastern Stikinia (Asitka Group; Ootes et al., in press). The Lay Range assemblage data consistently plot in the magmatic arc field above the mantle array.

being calved from a continental landmass, although we cannot rule out the possibility that the Lay Range arc developed immediately beyond the edge of a continental substrate (e.g., Ferri, 1997). If this landmass was a fragment of an older Paleozoic arc (e.g., Yukon-Tanana terrane; cf., Ferri, 1997), or a fragment of the Precambrian Shield of the North America, the Lay Range assemblage would contain diagnostic pre-Carboniferous detrital zircon population peaks, which it does not (Figs. 6f, 8a, b). Multi-cyclic reworking of older sedimentary deposits, such as described for example from the Mackenzie Mountains and Shaler supergroups (Rainbird et al., 2017) is an explanation for the range of non-overlapping Precambrian detrital zircons. We suggest that the peripheral landmass contained older sedimentary deposits that were reworked to generate second-cycle (or higher order) zircons found in the Lay Range assemblage.

Although the Mackenzie Mountains and Shaler supergroups (Meso- to Neoproterozoic) were deposited in northwest Laurentia, the characteristic Mesoproterozoic detrital zircons in these rocks (Fig. 12) were foreign to western Laurentian at the time of deposition. Grenville-aged zircons (1.5-1.0 Ga) in the Mackenzie Mountains Supergroup record a pan-continental drainage system that transported detritus eroded from the Grenville orogen more than 5000 km to the southeast (Rainbird et al., 2017). Similar population peaks in Cambrian sandstones of the Paleozoic passive margin reflect recycling of zircons that were liberated by erosion of Mackenzie Mountains Supergroup rocks (Cambrian Type II of Hadlari et al., 2012; Fig. 12).

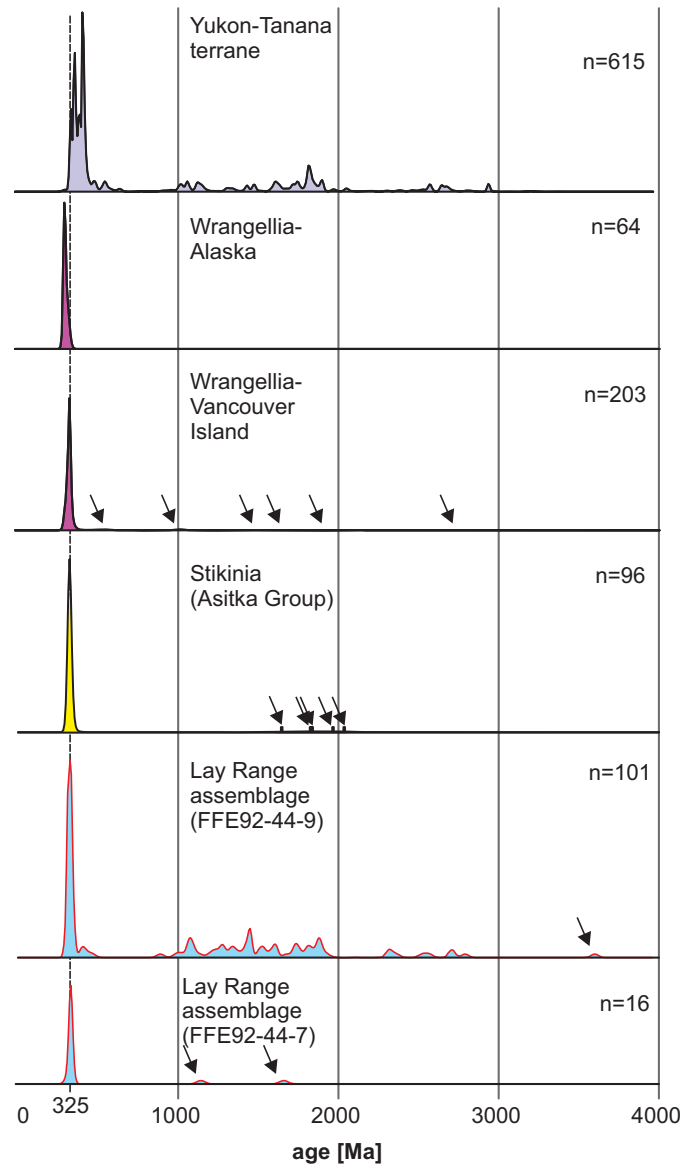


**Fig. 11.** Kernel density estimation plots of detrital zircon from the Yukon-Tanana terrane (Alaska, Pecha et al., 2016), Wrangellia (Alaska, Romero et al., 2020; Vancouver Island, Alberts et al., 2021), the Asitka Group of eastern Stikinia (Ootes et al., in press), and the Lay Range assemblage (this study). Arrows point to single (non-reproduced) zircon U-Pb results. Dashed vertical line at ca. 325 Ma demarcates the Carboniferous probability peak in each terrane, except Yukon-Tanana, which is older (450 to 350 Ma).

Similar recycling, with multiple episodes of deposition, uplift, erosion, and transport, likely accounts for the broad range of Precambrian detrital zircons in the Lay Range assemblage.

Possibly, Neoproterozoic through Cambrian passive margin deposits on the western margin of North America were the source of the detrital zircons. Importantly, the data (U-Pb and Hf systematics) do not support that erosion of the Yukon-Tanana terrane or Precambrian Shield provided sediment to this part of Quesnellia during the Carboniferous (cf., Ferri, 1997).

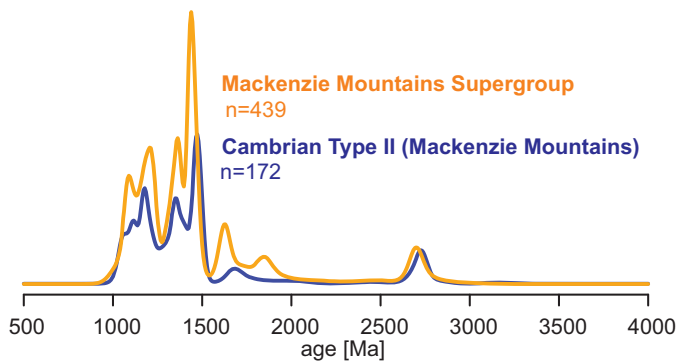


**Fig. 12.** Example of detrital zircons reworked through multiple sedimentary cycles. Comparison of detrital zircon probability distributions from the Mackenzie Mountains Supergroup (late Mesoproterozoic; Rainbird et al., 2017) and from Cambrian sandstones in the Mackenzie Mountains (Cambrian Type II of Hadlari et al., 2012). The Cambrian Type II sandstones display similar distributions with zircons having been derived from erosion of the Mackenzie Mountains Supergroup. Rather than representing first-cycle derivation from the original source rocks, the Cambrian Type II sandstones contain zircons that were temporarily stored in the Mackenzie Mountain Supergroup.

## 6. Conclusions

This study reports the biochronology and first detrital zircon U-Pb and Hf results from the Lay Range assemblage, the lowest stratigraphic unit exposed in north-central Quesnellia. Fossil evidence indicates deposition of the lower sedimentary division during the Late Mississippian to Middle Pennsylvanian and the upper mafic tuff division during the Middle Pennsylvanian to Permian. A quartz sandstone and a polymictic pebble conglomerate from the lower part of the lower sedimentary division yield detrital zircon U-Pb dates between 360 and 290 Ma (Carboniferous to early Permian), a range of older detrital zircons from 3600 to 890 Ma (Archean and Proterozoic) and a small population ( $n=4$ ) from 450 to 390 Ma (Ordovician to Devonian). The  $\epsilon_{\text{Hf}}(t)$  and trace element compositions of Carboniferous detrital zircons are consistent with the parental magma having formed in a juvenile arc. Lay Range zircon U-Pb,  $\epsilon_{\text{Hf}}(t)$ , and trace elements are comparable to those of the Asitka Group (eastern Stikinia) and Wrangellia but have little similarity to those of ancient North America or the Yukon-Tanana terrane. The older detrital zircons (Archean through Paleozoic) may have been sourced from a nearby continental oceanic plateau calved from a larger landmass that had little or no role in the genesis of the Carboniferous magmas. Recycling of zircons temporarily stored in older sedimentary deposits accounts for the large age spread of Precambrian detrital zircons in the Lay Range assemblage. Possibly, the postulated continental oceanic plateau may have rifted from western North American crust covered by Neoproterozoic through Cambrian passive margin deposits.

## Acknowledgments

This study is a contribution to the Hogen mapping project by the British Columbia Geological Survey. This is Natural Resources Canada contribution #20210442. Reviews by P. Schiarizza and S. Regan helped improved the manuscript.

## References cited

- Alberts, D., Gehrels, G.E., and Nelson, J.L., 2021. U-Pb and Hf analyses of detrital zircons from Paleozoic and Cretaceous strata on Vancouver Island, British Columbia: Constraints on the Paleozoic tectonic evolution of southern Wrangellia. *Lithosphere*, 7866944, 20 p. <<https://doi.org/10.2113/2021/7866944>>
- Allen, C.M., and Campbell, I.H., 2012. Identification and elimination of a matrix-induced systematic error in LA-ICP-MS  $^{206}\text{Pb}/^{238}\text{U}$  dating of zircon. *Chemical Geology*, 332-333, 157-165. <<https://doi.org/10.1016/j.chemgeo.2012.09.038>>
- Beatty, T.W., Orchard, M.J., and Mustard, P.S., 2006. Geology and tectonic history of the Quesnel terrane in the area of Kamloops, British Columbia. In Colpron, M., and Nelson, J.L., (Eds.), *Paleozoic Evolution and Metallogeny of Pericratonic Terranes at the Ancient Pacific Margin of North America, Canadian and Alaskan Cordillera*. Geological Association of Canada Special Paper 45, pp. 483-504.
- Ben-Avraham, Z., and Nur, A., 1983. An introductory overview to the concept of displaced terranes. *Canadian Journal of Earth Sciences*, 20, 994-999.
- Beranek, L.P., van Staal, C.R., McClelland, W.C., Israel, S., and Mihalyuk, M.G., 2013. Baltican crustal provenance for Cambrian-Ordovician sandstones of the Alexander terrane, North American Cordillera: evidence from detrital zircon U-Pb geochronology and Hf isotope geochemistry. *Journal of the Geological Society*, 170, 7-18.
- Bouvier, A., Vervoort, J.D., and Patchett, J.P., 2008. The Lu-Hf and Sm-Nd isotopic composition of CHUR: Constraints from unequilibrated chondrites and implications for the bulk composition of terrestrial planets. *Earth and Planetary Science Letters*, 273, 48-57.
- Chauvel, C., and Blichert-Toft, J., 2001. A hafnium isotope and trace element perspective on melting of the depleted mantle. *Earth and Planetary Science Letters*, 3-4, 137-151.
- Colpron, M., 2020. Yukon Terranes-A digital atlas of terranes for the northern Cordillera. Yukon Geological Survey. <<http://data.geology.gov.yk.ca/Compilation/2>> (accessed April 2021).
- Colpron, M., Nelson, J.L., and Murphy, D.C., 2007. Northern Cordilleran terranes and their interactions through time. *GSA Today*, 17, 4-10.
- Colpron, M., Crowley, J.L., Long, D.G.F., Murphy, D.C., Beranek, L., and Bickerton, L., 2015. Birth of the northern Cordilleran orogen, as recorded by detrital zircons in Jurassic synorogenic strata and regional exhumation in Yukon. *Lithosphere*, 7, 541-562.
- Coutts, D.S., Matthews, W.A., and Hubbard, S.M., 2019. Assessment of widely used methods to derive depositional ages from detrital zircon populations. *Geoscience Frontiers*, 10, 1421-1435. <<https://doi.org/10.1016/j.gsf.2018.11.002>>
- Davis, W.J., Ootes, L., Newton, L., Jackson, V.A., and Stern, R., 2015. Characterization of the Paleoproterozoic Hottah terrane, Wopmay Orogen using multi-isotopic (U-Pb, Hf and O) detrital zircon analyses: An evaluation of linkages to northwest Laurentian Paleoproterozoic domains. *Precambrian Research*, 269, 296-310. <<https://doi.org/10.1016/j.precamres.2015.08.012>>
- Ferri, F., 1997. Nina Creek Group and Lay Range Assemblage, north-central British Columbia: remnants of late Paleozoic oceanic and arc terranes. *Canadian Journal of Earth Sciences*, 34, 854-874.
- Ferri, F., 2000. Devonian-Mississippian Felsic Volcanism Along the Western Edge of the Cassiar Terrane, North-Central British Columbia. In: *Geological Fieldwork 1999, British Columbia Ministry of Energy and Mines, Paper 2000-1*, pp. 127-146.
- Ferri, F., Dudka, S.F., Rees, C.J., and Meldrum, D.G., 2001. Geology of the Aiken Lake Area north-central B.C. (NTS 94C/5, 6 & 12). British Columbia Ministry of Energy and Mines, British Columbia Geological Survey Geoscience Map 2001-10, scale 1:50,000.
- George, S.W.M., Nelson, J.L., Alberts, D., Greig, C.J., and Gehrels, G.E., 2021. Triassic-Jurassic accretionary history and tectonic

- origin of Stikinia from U-Pb geochronology and Lu-Hf isotope analysis, British Columbia. *Tectonics*, 40, e2020TC006505. <<https://doi.org/10.1029/2020TC006505>>
- Grimes, C.B., Wooden, J.L., Cheadle, M.J., and John, B.E., 2015. "Fingerprinting" tectono-magmatic provenance using trace elements in igneous zircon. *Contributions to Mineralogy and Petrology*, 170. <<https://doi.org/10.1007/s00410-015-1199-3>>
- Hadlari, T., Davis, W.J., Dewing, K., Heaman, L.M., Lemieux, Y., Ootes, L., Pratt, B.R., and Pyle, L.J., 2012. Two detrital zircon signatures for the Cambrian passive margin of northern Laurentia highlighted by new U-Pb results from northern Canada. *Geological Society of America Bulletin*, 124, 1155-1168.
- Harriott, T.M., Crowley, J.L., Schmitz, M.D., Wartes, M.A., and Gillis, R.J., 2019. Exploring the law of detrital zircon: LA-ICP-MS and CA-TIMS geochronology of Jurassic forearc strata, Cook Inlet, Alaska, USA. *Geology*, 47, 1044-1048.
- Ickert, R.B., 2013. Algorithms for estimating uncertainties in initial radiogenic isotope ratios and model ages. *Chemical Geology*, 340, 131-138.
- Johnsson, M.J., Stallard, R.F., and Lundberg, N., 1991. Controls on the composition of fluvial sands from a tropical weathering environment: Sands of the Orinoco River drainage basin, Venezuela and Columbia. *Geological Society of America Bulletin*, 103, 1622-1647.
- Malkowski, M.A., and Hampton, B.A., 2014. Sedimentology, U-Pb detrital geochronology, and Hf isotopic analyses from Mississippian-Permian stratigraphy of the Mystic subterrane, Farewell terrane, Alaska. *Lithosphere*, 6, 383-398. <<https://doi.org/10.1130/L365.1>>
- Monger, J.W.H., 1973. The Takla Group near Dewar Peak, McConnell Creek map-area (94D), British Columbia. *Geological Survey of Canada Paper 74-1B*, pp. 29-30.
- Monger, J.W.H., 1977. The Triassic Takla Group in McConnell Creek map-area, north-central British Columbia. *Geological Survey of Canada Paper 76-29*, 45 p.
- Monger, J.W.H., Wheeler, J.O., and Tipper, H.W., et al., 1991. Cordilleran Terranes. In: Gabrielse, H., and Yorath, C.J., (Eds.), *Geology of the Cordilleran Orogen in Canada*. Geological Survey of Canada, *Geology of Canada*, 4, 281-327.
- Monger, J.W.H., and Paterson, J.A., 1974. Upper Paleozoic and Lower Mesozoic Rocks of the Omineca Mountains. *Geological Survey of Canada Paper 74-1A*, pp. 19-20.
- Mortensen, J.K., Lucas, K., Monger, J.W.H., and Cordey, F., 2017. Synthesis of U-Pb and fossil age, lithochemical and Pb-isotopic studies of the Paleozoic basement of the Quesnel terrane in south-central British Columbia and northern Washington state. *Geoscience BC, Report 2017-1*, pp. 165-188.
- Nasdala, L., Lengauer, C.L., Hanchar, J.M., Kronz, A., Wirth, R., Blanc, P., Kennedy, A.K., and Seydoux-Guillaume, A.M., 2002. Annealing radiation damage and the recovery of cathodoluminescence. *Chemical Geology*, 191, 121-140.
- Ootes, L., Milidragovic, D., Friedman, R., Wall, C., Cordey, F., Luo, Y., Jones, G., Pearson, D.G., and Bergen, A., in press. Eastern Stikinia: No place for old basement? *Geosphere*.
- Ootes, L., Ferri, F., Milidragovic, D., and Wall, C., Detrital zircon data from the Lay Range assemblage and Vega Creek succession, north-central Quesnel terrane 2022. British Columbia Ministry of Energy, Mines and Low Carbon Innovation, British Columbia Geological Survey GeoFile.
- Paton, C., Hellstrom, J., Paul, B., Woodhead, J., and Hergt, J., 2011. Iolite: freeware for the visualization and processing of mass spectrometric data. *Journal of Analytical and Atomic Spectrometry*, 26, 2508-2518.
- Pecha, M.E., Gehrels, G.E., McClelland, W.C., Giesler, D., White, C., and Yokelson, I., 2016. Detrital zircon U-Pb geochronology and Hf isotope geochemistry of the Yukon-Tanana terrane, Coast Mountains, southeast Alaska. *Geosphere*, 12, 1556-1574.
- Rainbird, R.H., Rayner, N.M., Hadlari, T., Heaman, L.M., Ielpi, A., Turner, E.C., and MacNaughton, R.B., 2017. Zircon provenance data record the lateral extent of pancontinental, early Neoproterozoic rivers and erosional unroofing history of the Grenville orogen. *Geological Society of America Bulletin*, 129, 1408-1423.
- Romero, M.C., Ridgwah, K.D., and Gehrels, G.E., 2020. *Geology, U-Pb Geochronology, and Hf isotope geochemistry across the Mesozoic Alaska Range Suture Zone (South-Central Alaska): Implications for Cordilleran collisional processes and tectonic growth of North America*. *Tectonics*, 32. <<https://doi.org/10.1029/2019TC005946>>
- Roots, E.F., 1954. *Geology and mineral deposits of Aiken Lake map area, British Columbia*. Geological Survey of Canada, *Memoir 274*, 246 p.
- Ross, C.A., and Monger, J.W.H., 1978. Carboniferous and Permian Fusulinaceans from the Omineca Mountains, British Columbia. In: Donnelly, V., (Ed.), *Contributions to Canadian Paleontology*. Geological Survey of Canada *Bulletin 267*, pp. 43-63.
- Sun, S.S., and McDonough, W.F., 1989. Chemical and isotopic systematics of oceanic basalts: implications for mantle composition and processes. In: Saunders, A.D., and Norry, M.J., (Eds.), *Magmatism in the Ocean Basins*. Geological Society, London, *Special Publication 42*, 313-345.
- Vermeesch, P., 2018. IsoplotR: a free and open toolbox for geochronology. *Geoscience Frontiers*, 9, 1478-1493.
- Vervoort, J.D., and Kemp, A.I.S., 2016. Clarifying the zircon Hf isotope record of crust-mantle evolution. *Chemical Geology*, 425, 65-75.
- Woodhead, J., Hergt, J., Shelley, M., Eggins, S., and Kemp, R., 2004. Zircon Hf-isotope analysis with an excimer laser, depth profiling, ablation of complex geometries, and concomitant age estimation. *Chemical Geology*, 209, 121-135.